

# A Theoretical Analysis of Aniline-Based Dyes Structure Modification to Improve the Efficiency of Dye-Sensitized Solar Cells (DSSCs)

Imelda<sup>1,\*</sup>, Hermansyah Aziz<sup>1</sup>, Arxhel Septino Faril Nanda<sup>2</sup>, Elvira Deswita<sup>1</sup>

<sup>1</sup> Department of Chemistry, Faculty of Mathematics and Natural Science, Universitas Andalas, Padang, 25163, Indonesia

<sup>2</sup> Department of Informatics, Faculty of Information Technology, Universitas Andalas, Padang, 25163, Indonesia

\* Corresponding author: [imelda@sci.unand.ac.id](mailto:imelda@sci.unand.ac.id)

<https://doi.org/10.14710/jksa.28.9.481-487>

## Article Info

### Article history:

Received: 08<sup>th</sup> June 2025

Revised: 01<sup>st</sup> November 2025

Accepted: 05<sup>th</sup> November 2025

Online: 08<sup>th</sup> December 2025

### Keywords:

Aniline; D- $\pi$ -A; DFT; DSSCs

## Abstract

This study employed aniline-based D- $\pi$ -A organic dyes, consisting of four dyes differentiated by their  $\pi$ -conjugated moieties. Calculations were performed using DFT/TD-DFT with the B3LYP/6-31G basis set. The work examined structural modifications of aniline-based D- $\pi$ -A dyes in the gas phase to identify  $\pi$ -conjugated variations with high sensitizing potential for DSSCs. Among the dyes evaluated, Dye 2 (8-(4-aminophenyl)-9H-purine-2-carboxylic acid) showed the most promising characteristics, with an absorption maximum ( $\lambda_{\text{max}}$ ) of 504.45 nm and a bandgap of 3.0618 eV. These findings indicate that converting aniline dyes into D- $\pi$ -A systems can improve DSSC performance.

## 1. Introduction

Currently, renewable energy sources derive from continuous natural processes, including solar power, wind power, hydroelectric power, biofuels, biomass, and geothermal sources, and play a critical role in addressing the global energy crisis. Developed countries, such as the European Union, aim to achieve 27% of their total energy consumption from renewable sources by 2030. The United States has invested more than \$90 billion in developing clean energy through the Recovery Act [1].

In 1990, Grätzel and O'Regan introduced Dye-Sensitized Solar Cells (DSSCs) as the third-generation solar cell technology. DSSCs are low-cost, easy to fabricate, and capable of achieving high sunlight-to-electricity conversion efficiency [2]. Their core components include TiO<sub>2</sub> anode, a sensitizer, an I<sup>-</sup>/I<sub>3</sub><sup>-</sup> electrolyte, and a counter electrode. Sensitizer contributes crucially to improving light absorption efficiency [3, 4]. Sensitizers can be either organic or inorganic dyes. Ruthenium-based organometallic dyes are known to significantly enhance DSSC performance [5, 6], but their use is limited by high production costs due to the scarcity and expense of ruthenium [7]. Metal-free organic dyes offer several advantages, such as environmental friendliness, abundant availability,

structural tunability, low synthesis cost, and high molar extinction coefficients [8]. However, they generally exhibit lower light-absorption efficiency and stability, making structural modification necessary.

One type of organic dye is aniline, which occurs naturally in the *Indigofera suffruticosa* plant and can also be commercially produced through the hydrogenation of nitrobenzene [9]. Aniline has a simple molecular structure and contains a lone pair on its nitrogen atom, making it an effective electron donor [10]. However, aniline dyes require structural modification to enhance their performance in DSSCs. This improvement is typically achieved by converting aniline into D- $\pi$ -A (Donor- $\pi$ -conjugated-Acceptor) type dyes. D- $\pi$ -A dyes are highly suitable as DSSC sensitizers due to their strong push-pull electronic characteristics [11]. Previous studies on D- $\pi$ -A dyes have explored systems based on porphyrin [12], indoloquinoline and phenothiazine [13], aniline [14], triphenylamine [15], coumarin [16], quinoline [17], and others.

Charge transfer from the donor (D) to the acceptor (A) moiety occurs intramolecularly, and during photoexcitation, electrons are injected into the semiconductor's conduction band through the dye's acceptor unit. By modifying the donor, acceptor, and/or

$\pi$ -conjugated bridges, the absorption properties and excitation energies of the dye can be tuned, which can be effectively evaluated using computational methods [18, 19].

Computational methods now play a crucial role in scientific development, enabling the calculation of complex molecular properties with results that correlate strongly with experimental observations. These methods have become increasingly popular in recent years because they require less time and cost compared to laboratory experimentation. Among them, Density Functional Theory (DFT) is the most widely used due to its ability to produce accurate results that closely match experimental data [20].

Based on this background, this study focuses on a theoretical investigation of structural modifications of aniline-based dyes to enhance the performance of DSSCs. The objective is to characterize the  $\pi$ -conjugated variations of aniline-derived D- $\pi$ -A organic dyes and evaluate their potential for improving DSSC efficiency. Additionally, this work aims to identify the most favorable dye candidate to function as an efficient sensitizer in DSSCs.

## 2. Experimental

This study employed Gaussian 16W, using DFT for ground-state optimization and TD-DFT for excited-state optimization. The B3LYP/6-31G basis set was applied throughout the calculations [17]. All optimizations were performed in the gas phase. The molecular model used in this work consisted of D- $\pi$ -A type dyes, as shown in Figure 1. Molecular structures were constructed using GaussView 6.0. Each dye featured an aniline donor moiety and a formic acid acceptor moiety, combined with different  $\pi$ -conjugated bridge variations.

### 2.1. The Performance of DSSCs

The performance of DSSCs can be evaluated through key parameters, including the dye bandgap, short-circuit current density ( $J_{sc}$ ), open-circuit voltage ( $V_{oc}$ ), and overall energy conversion efficiency ( $\eta$ ). These parameters were analyzed using Equations (1–6). The ease of electron excitation in a dye is determined by the energy difference between the Highest Occupied Molecular Orbital (HOMO) and the Lowest Unoccupied Molecular Orbital (LUMO), commonly referred to as the bandgap [21] (Equation 1).

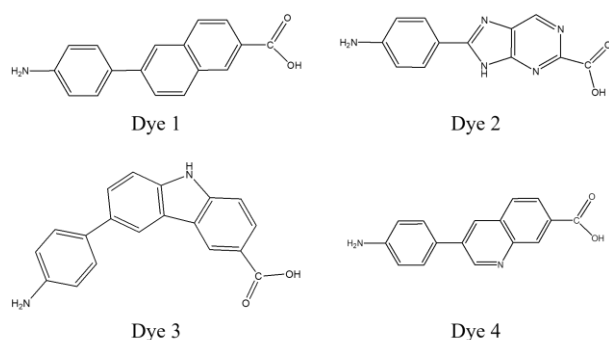


Figure 1. Dyes 1–4

$$\Delta E = E_{LUMO} - E_{HOMO} \quad (1)$$

A smaller bandgap enables electrons to be excited more easily from the HOMO to the LUMO, resulting in stronger light absorption. According to Planck's law, energy is inversely proportional to wavelength, meaning dyes with lower bandgaps absorb light more effectively [22]. The energy conversion efficiency of a DSSC is given by Equation 2.

$$\eta = \frac{J_{sc} \times V_{oc} (ff)}{I_s} \quad (2)$$

Where,  $J_{sc}$  is the short-circuit current density,  $V_{oc}$  is the open-circuit voltage,  $ff$  is the fill factor, and  $I_s$  is the light intensity. The  $V_{oc}$  of a DSSC reflects the energy difference between the redox potential of the electrolyte and the quasi-Fermi level of electrons in the TiO<sub>2</sub> conduction band [23] (Equations 3 and 4).

$$J_{sc} = \int \lambda LHE(\lambda) \times \Phi_{inject} \times \eta_{collect} \times d\lambda \quad (3)$$

$$V_{oc} = E_{LUMO} - E_{CB} \quad (4)$$

Where,  $ff$  is the fill factor,  $I_s$  is the light intensity,  $\Phi_{inject}$  is the electron injection efficiency,  $\eta_{collect}$  is the electron collection efficiency, and  $E_{CB}$  (conduction band energy of TiO<sub>2</sub>) value is -4.0 eV.

According to Equation 3, achieving a high  $J_{sc}$  requires large values of LHE (Light Harvesting Efficiency),  $\lambda$ , and  $\Phi_{inject}$ . LHE was calculated using Equation 5.

$$LHE = 1 - 10^{-f} \quad (5)$$

Where,  $f$  is the oscillator strength of dyes.

Electron injection free energy ( $\Delta G^{inject}$ ) was obtained using Equation 6.

$$\Delta G^{inject} = E_{dye^*} - E_{CB} = E_{dye} - E_{0-0} - E_{CB} \quad (6)$$

Where,  $E_{dye}$  is the oxidation potential of dyes in the basic state, and  $E_{0-0}$  is the vertical electronic transition energy in  $\lambda_{max}$  [24] or the bandgap of dyes [25].

## 3. Results and Discussion

### 3.1. Optimal Geometric Structures

The geometric structures of the four dyes with  $\pi$ -conjugated moiety variations were optimized using the B3LYP/6-31G basis set, aiming to obtain optimal structures and HOMO-LUMO contours of the dyes, as shown in Figure 2. The HOMO contours represent the electron density in the HOMO level, which reflects the electron-donating regions of the dye, while the LUMO contours represent the electron-accepting regions in the LUMO level [26]. In the HOMO, the electron density is distributed over the nitrogen atom of aniline, the C-C framework of the donor moiety, and part of the  $\pi$ -conjugated bridge, confirming that aniline functions as the electron-donating group. In the LUMO, the electron density is concentrated on the oxygen atoms of the formic acid unit and part of the  $\pi$ -bridge, indicating that formic acid acts as the electron-withdrawing group and the  $\pi$ -moiety serves as the electron-transfer pathway. Thus, upon sunlight exposure,  $\pi$ -electron resonance occurs from the aniline donor toward the formic acid acceptor.

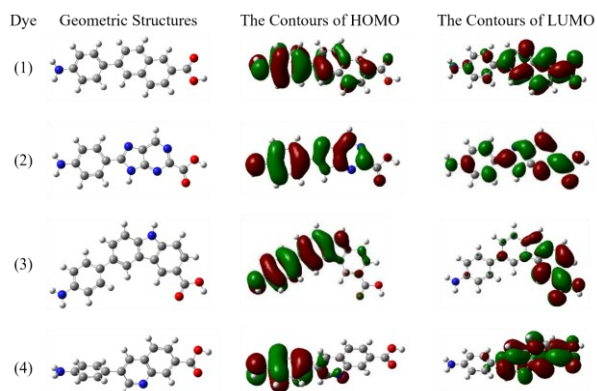


**Figure 2.** Optimal geometric structures of dyes 1–4 (atom colors: red = oxygen, blue = nitrogen, grey = carbon, white = hydrogen), contours of HOMO and LUMO

### 3.2. ESP (Electrostatic Surface Potential)

ESP analysis was used to identify the electronegative and electropositive regions within the dyes. Electronegativity refers to the ability of an atom, molecule, or ion to attract electrons toward itself [27]. The ESP color scale follows the order red > orange > yellow > green > blue, where red represents the most electronegative areas, and blue represents the most electropositive ones [28]. Electropositive regions (blue) act as electron donors, while electronegative regions (red) serve as electron acceptors. The ESP maps of dyes 1–4 in Figure 3 show that the formic acid group behaves as an electron-withdrawing region, whereas the amine group in aniline functions as an electron-donating region.

### 3.3. Frontier Energy and Bandgap ( $\Delta E$ )

In DSSCs, the source of electrical energy is the excitation of electrons on dyes. Electron excitation occurs from the HOMO to the LUMO bands, and the energy difference between the HOMO band and the LUMO bands is called the bandgap ( $\Delta E$ ). The efficient sensitizer in DSSCs has a small bandgap value; the smaller bandgap value facilitates the electron excitation from the HOMO to the LUMO bands. The data in Table 1 show the energy of HOMO–LUMO and the bandgap of dyes 1–4.

**Table 1.** The frontier energy of dyes 1–4

Dye	$\pi$ -conjugated	$E_{\text{HOMO}}$ (eV)	$E_{\text{LUMO}}$ (eV)	$\Delta E$ (eV)
Aniline	–	–5.10	0.06	5.16
1	naphthalene	–5.17	–1.85	3.33
2	purine	–5.40	–2.34	<b>3.06</b>
3	carbazole	–4.66	–1.49	3.18
4	quinoline	–5.36	–2.21	3.15

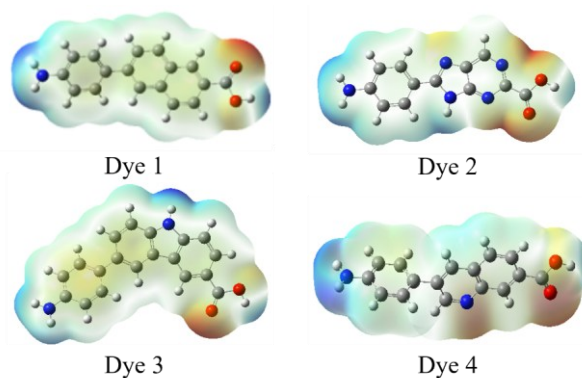


**Figure 3.** The ESP of dyes 1–4

Table 1 shows that all four dyes modified on the  $\pi$ -conjugated bridge have smaller bandgap values than the unmodified aniline. This indicates that the extended conjugation allows greater electron delocalization, making the HOMO–LUMO separation smaller and facilitating electronic excitation. A lower bandgap means that less light intensity is required to promote electrons from HOMO to LUMO [29]. Among the dyes, dye 2 has the smallest bandgap at 3.0618 eV. This is linked to the larger number of atoms in its  $\pi$ -conjugated purine moiety. Nitrogen atoms in the  $\pi$ -bridge have an electronegativity of 3.04, which is lower than that of oxygen (3.44) in the acceptor group [30], enabling the oxygen atoms to more effectively pull electron density from the nitrogen sites. At the same time, the nitrogen atoms, being more electronegative than the carbon atoms in the donor region, readily attract electrons from the donor moiety. This overall gradient in electronegativity enhances intramolecular charge transfer within dye 2, resulting in a reduced bandgap.

### 3.4. Dihedral Angle and Bond Length

The bond lengths and dihedral angles of dyes 1–2 are summarized in Table 2. In DSSCs, the geometric structure of the dye significantly influences its electronic and optical properties. Two key structural parameters are the dihedral angle and bond length. The dihedral angle reflects the planarity of the molecular moieties; values approaching  $0^\circ$  or  $180^\circ$  indicate a coplanar arrangement, which facilitates more efficient electron transfer between moieties. Likewise, shorter bond lengths promote easier electron movement along the molecular framework [25].

**Table 2.** The dihedral angle ( $\theta$ ) and bond length ( $d$ ) of dyes 1–4

Dye	$\theta_1$ ( $^\circ$ )	$\theta_2$ ( $^\circ$ )	$d_1$ (Å)	$d_2$ (Å)
1	–37.02	–0.09	1.48	1.45
2	<b>0.00055</b>	<b>–179.98</b>	<b>1.44</b>	<b>1.43</b>
3	–158.90	–0.01	1.46	1.43
4	90.31	0.00083	1.48	1.44

In Table 2,  $\theta_1$  and  $d_1$  represent the dihedral angle and bond length between the donor moiety and the  $\pi$ -conjugated bridge, while  $\theta_2$  and  $d_2$  represent those between the  $\pi$ -conjugated bridge and the acceptor moiety. Based on the data, dye 2 shows a dihedral angle closer to  $0^\circ$  and shorter bond lengths compared to the other dyes. This structural arrangement promotes more efficient electron transfer, indicating that dye 2 has the most favorable geometry for charge transport.

### 3.5. Absorption Spectrum

The absorption spectra of dyes 1–4 are shown in Figure 4, and their electronic transitions are summarized in Table 3. In the spectrum, the X-axis represents the wavelength, while the Y-axis corresponds to the molar absorptivity ( $\epsilon$ ). As seen in Figure 4, dye 1 exhibits the highest molar absorptivity, whereas dye 2 shows stronger absorption at longer wavelengths than the other dyes.

Table 3 shows that all modified dyes exhibit longer wavelength absorption than aniline. Their absorption wavelengths fall within the visible region, with dye 2 displaying the highest value at 504.45 nm, along with the lowest excitation energy of 2.4578 eV. The electronic transitions are dominated by major contributions from  $H \rightarrow L$ ,  $H \rightarrow L+1$ ,  $H-1 \rightarrow L$ ,  $H \rightarrow L+2$ , and  $H \rightarrow L+1$ , while minor

transitions appear in bands such as  $H-2 \rightarrow L$ ,  $H-1 \rightarrow L+1$ ,  $H-3 \rightarrow L$ , and  $H-1 \rightarrow L+3$ .

A dye with strong light absorption efficiency generally shows both high intensity and broad wavelength coverage. However, wavelength plays a more decisive role in enhancing DSSC performance [31]. Based on these parameters, dye 2 is the most efficient sensitizer among the investigated dyes.

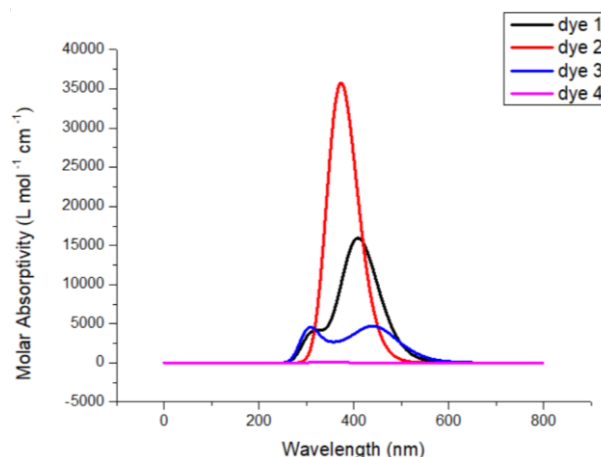


Figure 4. The UV-Vis spectra of dyes 1–4

Table 3. The data of electronic transitions of dyes 1–4

Dye	Excitation condition	$\lambda_{\text{excitation}}$ (nm)	Excitation (eV)	The configuration of the molecular orbital	Oscillator strength (f)
Aniline	1	273.98	4.5254	$H-1 \rightarrow L+1$ (30.17 %) $H \rightarrow L$ (95.38 %)	0.0447
	2	217.12	5.7103	$H-1 \rightarrow L$ (44.38 %) $H \rightarrow L+1$ (89.23 %)	0.1059
	3	198.12	6.2579	$H \rightarrow L+2$ (99.64 %)	0.0005
1	1	409.44	3.0281	$H \rightarrow L$ (99.16 %)	0.3900
	2	336.95	3.6796	$H-2 \rightarrow L$ (24.72 %) $H-1 \rightarrow L$ (76.26 %) $H \rightarrow L+1$ (56.47 %)	0.0422
	3	308.22	4.0226	$H-1 \rightarrow L$ (58.94 %) $H \rightarrow L+1$ (56.47 %)	0.0739
2	1	504.45	2.4578	$H-1 \rightarrow L$ (98.95 %)	0.0001
	2	373.01	3.3239	$H \rightarrow L$ (99.48 %)	0.8825
	3	330.06	3.7564	$H-3 \rightarrow L$ (31.72 %) $H-1 \rightarrow L+1$ (87.53 %) $H-1 \rightarrow L+3$ (3.01 %)	0.0015
3	1	444.95	2.7865	$H \rightarrow L$ (99.20 %)	0.1099
	2	367.40	3.3747	$H-2 \rightarrow L$ (14.86 %) $H \rightarrow L+1$ (97.39 %)	0.0486
	3	306.90	4.0399	$H-2 \rightarrow L$ (38.34 %) $H-2 \rightarrow L+1$ (16.98 %) $H-1 \rightarrow L$ (83.06 %) $H \rightarrow L+2$ (32.08 %)	0.1090
4	1	474.13	2.6150	$H \rightarrow L$ (99.10 %)	0.0003
	2	348.61	3.5566	$H-2 \rightarrow L$ (97.70 %)	0.0017
	3	332.85	3.7249	$H \rightarrow L+1$ (98.33 %)	0.0010

Note: H refers to the HOMO (Highest Occupied Molecular Orbital), and L refers to the LUMO (Lowest Unoccupied Molecular Orbital).



### 3.6. Dipole Moment and $\Delta G^{\text{inject}}$ Injected Gibbs Free Energy

Table 4 presents the dipole moment and  $\Delta G^{\text{inject}}$  values of dyes 1–4. The dipole moment reflects the degree of polarization within a molecule; a higher value indicates that the molecule polarizes more easily [32]. In D- $\pi$ -A dyes, polarization leads to a positive pole on the donor moiety and a negative pole on the acceptor moiety as electrons move through the  $\pi$ -conjugated bridge. A larger dipole moment generally facilitates electron transfer from donor to acceptor. Among the studied dyes, dye 4 shows the highest dipole moment, whereas dye 2 has a notably lower value due to the presence of multiple nitrogen atoms within its  $\pi$ -conjugated bridge, which distributes polarity across the structure. This indicates that the dipole moment alone is not the primary determinant of  $\pi$ -electron resonance in these dyes [33].

All modified aniline-based D- $\pi$ -A dyes exhibit higher dipole moments than unmodified aniline.  $\Delta G^{\text{inject}}$  indicates the spontaneity of electron injection, where more negative values correspond to more favorable injection processes. Dye 4 shows the most spontaneous  $\Delta G^{\text{inject}}$ , although the values for dyes 1 and 2 are only slightly less negative. Overall, dyes 1, 2, and 4 all demonstrate favorable electron injection characteristics for DSSC applications.

### 3.7. Electrical Properties Analysis

The capability of dyes to produce electrical current is evaluated through key electrical parameters, such as the values of  $V_{\text{oc}}$ ,  $J_{\text{sc}}$ , and  $\eta$ . A high value of  $\eta$  is achieved when both  $V_{\text{oc}}$  and  $J_{\text{sc}}$  are high while the light intensity remains low, as described in Equation 5.

**Table 4.** Dipole moment and  $\Delta G^{\text{inject}}$  of dyes 1–4

Dye	$\pi$ -conjugated	Dipole moment (D)	$\Delta G^{\text{inject}}$ (eV)
Aniline	-	4.08	-6.26
1	naphthalene	22.49	-4.50
2	purine	07.62	-4.46
3	carbazole	23.01	-3.84
4	quinoline	28.83	-4.51

**Table 5.** The values of LHE and  $V_{\text{oc}}$  of dyes 1–4

Dye	$\pi$ - conjugated	LHE	$V_{\text{oc}}$ (eV)
1	naphthalene	0.5926, 0.0926, 0.1565	2.1526
2	purine	0.0002, 0.8689, 0.0034	1.6647
3	carbazole	0.2236, 0.1059, 0.2220	2.5145
4	quinoline	0.0007, 0.0039, 0.0023	1.7874

According to Equation 2, the  $\eta$  value increases when the light intensity decreases. Lower light intensity corresponds to higher wavelengths.  $J_{\text{sc}}$  represents the current density per 1 cm<sup>2</sup> of cell area, and based on Equation 3, it is influenced by the values of LHE and  $\lambda$ . Higher LHE and longer wavelengths will lead to a higher  $J_{\text{sc}}$  value. As shown in Table 5, dye 2 has the highest LHE value.

The  $V_{\text{oc}}$  reflects the amount of energy delivered across the cell; a longer electron transport domain produces a higher voltage, resulting in a higher  $V_{\text{oc}}$  value [3]. Table 5 shows that dye 3 has the highest  $V_{\text{oc}}$ . However, among these parameters, the most influential factor for electrical energy efficiency is the wavelength absorption capability of the dye. Therefore, dye 2 is predicted to exhibit superior light-harvesting efficiency and overall DSSC energy conversion efficiency.

## 4. Conclusion

According to the analysis of the conducted study on aniline-based D- $\pi$ -A type organic dyes with the modification of the  $\pi$ -conjugated moiety through the DFT/TD-DFT method with a basis set of B3LYP/6-31G, the density in the contours of HOMO was formed in the domain of the electron donor, while the density in the contours of LUMO was formed in the domain of the electron acceptor. According to the parameters of bandgap value, the absorption of wavelength, excitation energy, oscillator strength, LHE, dihedral angle, and bond length, dye 2, named 8-(4-aminophenyl)-9H-purine-2-carboxylic acid, exhibits the most favorable properties, including an absorption maximum ( $\lambda$ ) of 504.45 nm. These values indicate that the latest aniline-based dye is capable of improving the efficiency of light absorption in DSSC equipment.

## References

- [1] Jiawei Gong, K. Sumathy, Qiquan Qiao, Zhengping Zhou, Review on dye-sensitized solar cells (DSSCs): Advanced techniques and research trends, *Renewable and Sustainable Energy Reviews*, 68, (2017), 234–246 <https://doi.org/10.1016/j.rser.2016.09.097>
- [2] Brian O'Regan, Michael Grätzel, A low-cost, high-efficiency solar cell based on dye-sensitized colloidal TiO<sub>2</sub> films, *Nature*, 353, 6346, (1991), 737–740 <http://doi.org/10.1038/353737a0>
- [3] I. N. Obotowo, I. B. Obot, U. J. Ekpe, Organic sensitizers for dye-sensitized solar cell (DSSC): Properties from computation, progress and future perspectives, *Journal of Molecular Structure*, 1122, (2016), 80–87 <https://doi.org/10.1016/j.molstruc.2016.05.080>
- [4] Abdul Qaiyum Ramle, Hamid Khaleedi, Ameerul Hazeq Hashim, Muhammad Ammar Mingsukang, Abdul Kariem Mohd Arof, Hapipah Mohd Ali, Wan Jeffrey Basirun, Indolenine – dibenzotetraaza [14] annulene Ni (II) complexes as sensitizers for dye - sensitized solar cells, *Dyes and Pigments*, 164, (2019), 112–118 <https://doi.org/10.1016/j.dyepig.2019.01.009>
- [5] Said Kerraj, Ahmed Arif, Younes Rachdi, Abdelkhalk Aboulouard, Mohammed Salah, Mohammed El idrissi, Said Belaaouad, Exploring the optoelectronic

- and photovoltaic properties of Ru-Arene complexes: DFT and TD-DFT insights into DSSC performance, *Journal of Organometallic Chemistry*, 1034, (2025), 123650  
<https://doi.org/10.1016/j.jorganchem.2025.123650>
- [6] Said Kerraj, Amine Harbi, Kassem El Mecherfi, Mohamed Moussaoui, Mohammed Salah, Said Belaouad, Moutaabbid Mohammed, Computational analysis of ligand design for Ru half-sandwich sensitizers in bulk heterojunction (BHJ) solar cells: Exploring the role of  $-NO_2$  group position and  $\pi$ -conjugation in optimizing efficiency, *Journal of the Indian Chemical Society*, 101, 5, (2024), 101148  
<https://doi.org/10.1016/j.jics.2024.101148>
  - [7] Said Kerraj, Mohamed Moussaoui, Younes Rachdi, Ahmed Arif, Mohamed Kadour Atouailaa, Khadijah M. Al-Zaydi, Abdelkhalk Aboulouard, Mohammed Salah, Said Belaouad, Mohammed El idrissi, Computational study of the optoelectronic and photovoltaic properties of arene-functionalized chromium complexes as sensitizers for enhancing DSSC performance, *Polyhedron*, 279, (2025), 117618  
<https://doi.org/10.1016/j.poly.2025.117618>
  - [8] Praveen Naik, Rui Su, Mohamed R. Elmorsy, Ahmed El-Shafei, Airody Vasudeva Adhikari, New carbazole based dyes as effective co-sensitizers for DSSCs sensitized with ruthenium (II) complex (NCSU-10), *Journal of Energy Chemistry*, 27, 2, (2018), 351-360  
<https://doi.org/10.1016/j.jechem.2017.12.013>
  - [9] Rute Caetano, Maria Amélia Lemos, Francisco Lemos, Filipe Freire, Modeling and control of an exothermal reaction, *Chemical Engineering Journal*, 238, (2014), 93-99  
<https://doi.org/10.1016/j.cej.2013.09.113>
  - [10] Mao Liang, Jun Chen, Arylamine organic dyes for dye-sensitized solar cells, *Chemical Society Reviews*, 42, 8, (2013), 3453-3488  
<https://doi.org/10.1039/C3CS35372A>
  - [11] Anup Pramanik, Sunandan Sarkar, Sougata Pal, Pranab Sarkar, Pentacene-fullerene bulk-heterojunction solar cell: A computational study, *Physics Letters A*, 379, 14-15, (2015), 1036-1042  
<https://doi.org/10.1016/j.physleta.2015.01.040>
  - [12] Haoran Zhou, Jung-Min Ji, Sung Ho Kang, Min Su Kim, Hyun Seok Lee, Chul Hoon Kim, Hwan Kyu Kim, Molecular design and synthesis of D- $\pi$ -A structured porphyrin dyes with various acceptor units for dye-sensitized solar cells, *Journal of Materials Chemistry C*, 7, 10, (2019), 2843-2852  
<http://doi.org/10.1039/C8TC05283B>
  - [13] Xing Qian, Xiaoying Wang, Li Shao, Hongmei Li, Rucai Yan, Linxi Hou, Molecular engineering of D- $\pi$ -A type organic dyes incorporating indoloquinoline and phenothiazine for highly efficient dye-sensitized solar cells, *Journal of Power Sources*, 326, (2016), 129-136  
<https://doi.org/10.1016/j.jpowsour.2016.06.127>
  - [14] I. Duerto, E. Colom, J. M. Andrés-Castán, S. Franco, J. Garín, J. Orduna, B. Villacampa, M. J. Blesa, DSSCs based on aniline derivatives functionalized with a tert-butyltrimethylsilyl group and the effect of the  $\pi$ -spacer, *Dyes and Pigments*, 148, (2018), 61-71  
<https://doi.org/10.1016/j.dyepig.2017.07.063>
  - [15] Liezel L. Estrella, Sang Hee Lee, Dong Hee Kim, New semi-rigid triphenylamine donor moiety for D- $\pi$ -A sensitizer: Theoretical and experimental investigations for DSSCs, *Dyes and Pigments*, 165, (2019), 1-10  
<https://doi.org/10.1016/j.dyepig.2019.02.002>
  - [16] Nitesh N. Ayare, Suryapratap Sharma, Keval K. Sonigara, Jyoti Prasad, Saurabh S. Soni, Nagaiyan Sekar, Synthesis and computational study of coumarin thiophene-based D- $\pi$ -A azo bridge colorants for DSSC and NLOphoric application, *Journal of Photochemistry and Photobiology A: Chemistry*, 394, (2020), 112466  
<https://doi.org/10.1016/j.jphotochem.2020.112466>
  - [17] Rajaa Diany, Said Kerraj, Abdelkhalk Aboulouard, Asad Syed, Abdellah Zeroual, Ali H. Bahkali, Mohamed El Idrissi, Mohammed Salah, Abdessamad Tounsi, Enhancing dye sensitized solar cells performance through quinoxaline based organic dye sensitizers, *Journal of Computational Electronics*, 23, 6, (2024), 1195-1208  
<https://doi.org/10.1007/s10825-024-02211-3>
  - [18] Panida Surawatanawong, Aleksander K. Wójcik, Supavadee Kiatisevi, Density functional study of mono-branched and di-branched di-anchoring triphenylamine cyanoacrylic dyes for dye-sensitized solar cells, *Journal of Photochemistry and Photobiology A: Chemistry*, 253, (2013), 62-71  
<https://doi.org/10.1016/j.jphotochem.2012.12.020>
  - [19] Kassem El Mecherfi, Said Kerraj, Rajaa Diany, Abdeljabbar Jaddi, Mohammad Shahidul Islam, Tahani Mazyad Almutairi, Abdelaziz Amine, Rkia Zari, Habib El Alaoui El Abdellaoui, Mohammed Salah, Harnessing sunlight with porphyrins: A quantum and impedance spectroscopy study for DSSCs, *Journal of the Indian Chemical Society*, 102, 8, (2025), 101863  
<https://doi.org/10.1016/j.jics.2025.101863>
  - [20] Zhu-Zhu Sun, Quan-Song Li, Min Zhang, Ze-Sheng Li, Exploring the regeneration process of ruthenium(II) dyes by cobalt mediator in dye-sensitized solar cells from first-principle calculations, *Journal of Power Sources*, 294, (2015), 264-271  
<https://doi.org/10.1016/j.jpowsour.2015.06.094>
  - [21] Chengyou Wang, Jing Li, Shengyun Cai, Zhijun Ning, Dongmei Zhao, Qiong Zhang, Jian-Hua Su, Performance improvement of dye-sensitizing solar cell by semi-rigid triarylamine-based donors, *Dyes and Pigments*, 94, 1, (2012), 40-48  
<https://doi.org/10.1016/j.dyepig.2011.11.002>
  - [22] V. Nadtochenko, N. Denisov, A. Gorenberg, Yu Kozlov, P. Chubukov, J. A. Rengifo, C. Pulgarin, J. Kiwi, Correlations for photocatalytic activity and spectral features of the absorption band edge of  $TiO_2$  modified by thiourea, *Applied Catalysis B: Environmental*, 91, 1-2, (2009), 460-469  
<https://doi.org/10.1016/j.apcatb.2009.06.015>
  - [23] Tannia Marinado, Kazuteru Nonomura, Jarl Nissfolk, Martin K. Karlsson, Daniel P. Hagberg, Licheng Sun, Shogo Mori, Anders Hagfeldt, How the Nature of Triphenylamine-Polyene Dyes in Dye-Sensitized Solar Cells Affects the Open-Circuit Voltage and Electron Lifetimes, *Langmuir*, 26, 4, (2010), 2592-2598  
<http://doi.org/10.1021/la902897z>
  - [24] Hongbo Wang, Qian Liu, Dejiang Liu, Runzhou Su, Jinglin Liu, Yuanzuo Li, Computational Prediction of

Electronic and Photovoltaic Properties of Anthracene-Based Organic Dyes for Dye-Sensitized Solar Cells, 2018, 1, (2018), 4764830  
<https://doi.org/10.1155/2018/4764830>

- [25] Rakesh Dutta, Shahnaz Ahmed, Dhruva Jyoti Kalita, Theoretical design of new triphenylamine based dyes for the fabrication of DSSCs: A DFT/TD-DFT study, *Materials Today Communications*, 22, (2020), 100731  
<https://doi.org/10.1016/j.mtcomm.2019.100731>
- [26] Imelda, Emriadi, Hermansyah Aziz, Adlis Santoni, Nofitri Utami, The Modification of Cyanidin Based Dyes to Improve The Performance of Dye-Sensitized Solar Cells (DSSCs), *Rasayan Journal of Chemistry*, 13, 1, (2020), 121–130  
<http://dx.doi.org/10.31788/RJC.2019.1245449>
- [27] Miloslav Nič, Jiří Jiráť, Bedřich Košata, Aubrey Jenkins, Alan McNaught, *IUPAC Compendium of Chemical Terminology*, IUPAC, Research Triangle Park, NC, 2009, <sup>^</sup><http://doi.org/10.1351/goldbook>
- [28] Yuanchao Li, Jingyan Liu, Dixin Liu, Xin Li, Yanling Xu, D-A-  $\pi$  -A based organic dyes for efficient DSSCs: A theoretical study on the role of  $\pi$  -spacer, *Computational Materials Science*, 161, (2019), 163–176  
<https://doi.org/10.1016/j.commatsci.2019.01.033>
- [29] Renee Kroon, Martijn Lenes, Jan C. Hummelen, Paul W. M. Blom, Bert de Boer, Small Bandgap Polymers for Organic Solar Cells (*Polymer Material Development in the Last 5 Years*), *Polymer Reviews*, 48, 3, (2008), 531–582  
<https://doi.org/10.1080/15583720802231833>
- [30] Imelda, Emriadi, Hermansyah Aziz, Adlis Santoni, Rifno Gusfri Ramadhan, Riska Astin Fitria, Theoretical Investigation of Aniline-Based Dyes to Improve The Efficiency of Solar Cells, *SSRG International Journal of Applied Chemistry*, 7, 2, (2020), 75–80  
<https://doi.org/10.14445/23939133/IJAC-V7I2P111>
- [31] D. D. Pratiwi, F. Nurosyid, A. Supriyanto, R. Suryana, Performance improvement of dye-sensitized solar cells (DSSC) by using dyes mixture from chlorophyll and anthocyanin, *Journal of Physics: Conference Series*, 2017 <http://doi.org/10.1088/1742-6596/909/1/012025>
- [32] P. Senthilkumar, C. Nithya, P. M. Anbarasan, Quantum chemical investigations on the effect of dodecyloxy chromophore in 4-amino stilbene sensitizer for DSSCs, *Spectrochimica Acta Part A: Molecular and Biomolecular Spectroscopy*, 122, (2014), 15–21 <https://doi.org/10.1016/j.saa.2013.11.023>
- [33] Bo Liu, Xiaoyan Li, Miaoyin Liu, Zhijun Ning, Qiong Zhang, Chen Li, Klaus Müllen, Weihong Zhu, Photovoltaic performance of solid-state DSSCs sensitized with organic isophorone dyes: Effect of dye-loaded amount and dipole moment, *Dyes and Pigments*, 94, 1, (2012), 23–27  
<https://doi.org/10.1016/j.dyepig.2011.11.005>